cosmetics

MDPI

Article

A Novel In Vitro Dry Skin Model Using Minipig and Human Cadaver Skin for Evaluating Moisturizer Efficacy

Ji-Woo Choe [1,2], Bae-Gon Kang [3], Jeong-hyun Hong [1,2], Kwanghyeon Liu [3] and Kyung-Min Lim [1,2,*]

1 College of Pharmacy, Graduate School of Pharmaceutical Sciences, Ewha Womans University, Seoul 03760, Republic of Korea; ch02j1w00@naver.com (J.-W.C.); hongjh126@gmail.com (J.-h.H.)
2 Graduate Program in Innovative Biomaterials Convergence, Ewha Womans University, Seoul 03760, Republic of Korea
3 BK21 FOUR Community-Based Intelligent Novel Drug Discovery Education Unit, College of Pharmacy and Research Institute of Pharmaceutical Sciences, Kyungpook National University, Daegu 41566, Republic of Korea; baegon0709@naver.com (B.-G.K.); dstlkh@knu.ac.kr (K.L.)
* Correspondence: kmlim@ewha.ac.kr

Abstract

Moisturizers are key components of skincare products, and reliable test methods are essential for evaluating their barrier-repairing and hydrating efficacy. However, the viscous and waxy nature of many cosmetic moisturizers limits the applicability of conventional cell-based in vitro assays. In this study, we developed a novel in vitro dry skin model using epidermal sheets from minipig and human cadaver skin—models widely accepted in skin absorption research. To simulate dry skin conditions, various stimuli were applied, including the lipid-extracting solvent tert-butyl methyl ether (MTBE; 100%), 50/50 MTBE/Acetone solution (M/A), the irritant surfactant sodium dodecyl sulfate (SDS; 1%), ultraviolet B (UVB) irradiation (30 mJ/cm^2), and tape stripping. Skin barrier disruption and stratum corneum damage were evaluated by assessing epidermal lipid integrity, histological alterations, transepidermal water loss (TEWL), and FITC-dextran permeation. All treatments induced significant dry skin conditions, as evidenced by disrupted lipid architecture, histological damage, and increased TEWL and FITC-dextran flux. Among them, M/A applied for 5 min produced the most consistent and reproducible changes across parameters. This protocol also yielded comparable results in human cadaver skin, supporting its applicability for evaluating the skin barrier-protective effects of cosmetic ingredients.

Keywords: dry skin model; moisturizer; in vitro test method

check for updates

Academic Editor: Nobutomo Ikarashi

Received: 16 July 2025
Revised: 3 September 2025
Accepted: 12 September 2025
Published: 16 September 2025

Citation: Choe, J.-W.; Kang, B.-G.; Hong, J.-h.; Liu, K.; Lim, K.-M. A Novel In Vitro Dry Skin Model Using Minipig and Human Cadaver Skin for Evaluating Moisturizer Efficacy. *Cosmetics* **2025**, *12*, 203. https://doi.org/10.3390/cosmetics12050203

Copyright: © 2025 by the authors. Licensee MDPI, Basel, Switzerland. This article is an open access article distributed under the terms and conditions of the Creative Commons Attribution (CC BY) license (https://creativecommons.org/licenses/by/4.0/).

1. Introduction

Recent interest in skin health has driven to rapid growth in the cosmetics industry [1]. Among the key functionalities of skincare products, moisturization is increasingly recognized as fundamental to the maintenance of skin health [2,3]. Consumers widely use skin moisturizers to retain youthful, hydrated skin and to prevent dryness [4]. These products play a critical role in preventing transepidermal water loss (TEWL) and replenishing skin hydration [5–8]. By doing so, they help preserve the integrity of the skin barrier and reduce the risk of skin disorders such as xerosis, inflammation, and wrinkle formation [9,10]. As a result, moisturizers are incorporated into a broad range of cosmetic formulations—including lotions, creams, and serums—and the demand for novel and effective moisturizing agents continues to grow [11,12].

The integrity of the stratum corneum (SC) is central to maintaining skin hydration. Disruption of the SC by exogenous factors leads to increased TEWL and alters the composition of lipids and proteins within the barrier [13–15]. The SC's lipid bilayers—primarily composed of ceramides, cholesterol, and fatty acids—are critical for its barrier function. External agents such as surfactants and organic solvents can extract these lipids or disrupt bilayer structure, resulting in skin barrier impairment and associated conditions like xerosis and dermatitis [16,17]. Ultraviolet (UV) radiation is another key factor that compromises SC function, promoting photoaging via DNA damage and oxidative stress pathway [18,19]. Mechanical factors such as scratching or friction also degrade the SC, increasing skin sensitivity and vulnerability to irritants, allergens, and pathogens [20,21]. This cascade of damage can further aggravate dry skin conditions through inflammation and immune activation.

To support the development of novel moisturizing agents, robust and reliable experimental models are essential for evaluating their efficacy. However, conventional in vitro cell-based assays are often unsuitable due to the high viscosity and waxy nature of many cosmetic moisturizers. Moreover, such models fail to accurately replicate key functional endpoints—such as TEWL and barrier recovery—that are central to moisturizer efficacy. Consequently, current evaluation approaches largely rely on clinical studies in human subjects [22–24]. These studies, while informative, suffer from inherent variability and require stringent environmental control and large sample sizes to ensure statistical power [25–28].

There is a growing need for experimental models that better simulate dry skin architecture, allow for application of viscous formulations, and enable quantitative evaluation of skin barrier function [29,30]. Several alternatives have been explored, including three-dimensional reconstructed human epidermis models [31], and ex vivo skin tissues from humans or pigs [32–35]. These models can support analyses such as TEWL, fluorescence-based permeability assays, immunostaining, and histological examination [36–38]. However, limitations such as high cost, inter-batch variability, limited supply, and short storage duration hinder their broad utility.

In this study, we established a dry skin model using isolated minipig epidermis and human cadaver skin, which can be stored under refrigerated conditions for extended periods and is relatively cost-effective. These skin tissues were subjected to controlled physical and chemical insults to induce SC disruption and simulate dry skin conditions. Our results demonstrate that this in vitro model provides a practical and reproducible platform to evaluate the barrier-protective effects of moisturizing agents, offering a valuable alternative to clinical trials and existing in vitro systems.

2. Materials and Methods

2.1. Skin Tissues

Minipig epidermis was obtained from Apures Co. (Gyeonggi, Republic of Korea) and consists of minipig back skin. For the experiments, tissue samples of two sizes were used: 15 mm × 15 mm × 300 μm, and 25 mm × 25 mm × 500 μm. The minipig skin was delivered in a frozen state and stored at −20 °C and all experiments were conducted within 6 months after the animal sacrifice. Prior to use, the samples were thawed at room temperature for 30 min and then stabilized by incubation in PBS at 37 °C for 20 min.

Human cadaver full skin (epidermis and dermis) was obtained from Seed group Derma:LabTM (Seoul, Republic of Korea). For the experiments, tissue samples of female trunk skin, measuring 30 mm × 30 mm × 1 mm, were used. These samples were delivered frozen and stored at temperatures between −20 °C and −40 °C and were used for experiments within 2 years of donation. Before use, the samples were thawed at room temperature for 10 min without undergoing any additional stabilization process.

To ensure the quality of tissue prior to experimentation, TEWL was measured for each skin sample. Tissues exhibiting values exceeding the threshold of 40 g/h·m^2 were considered compromised and excluded from subsequent analyses.

2.2. Dry Skin Conditions

For drying conditions, UVB at 30 mJ/cm^2 was irradiated using the UV Irradiation System—Bio-Sun (Vilber, Suebia, Germany) at the specified intensity. For tape stripping, the tissue was secured with forceps while tape segments (Scotch™, 3M, St. Paul, MN, USA) were applied and removed to mechanically detach the stratum corneum. This process was repeated 100 times, with the tape replaced every 10 applications. For chemical-induced drying, 20 µL of the chemical solution per 1 cm^2 was applied to either minipig epidermis or human cadaver skin. The 50/50 MTBE/Acetone solution (M/A) was prepared by mixing MTBE and acetone at a 1:1 ratio, and the 1% SDS solution was diluted in H_2O. Two exposure durations (1 and 5 min) were employed, and after treatment, the samples were washed with PBS to remove any residual chemicals.

2.3. Nile Red Staining

Skin sections were stained with Nile Red to visualize the lipid distribution in the stratum corneum. The staining solution was prepared by diluting 15–20 µL of Nile Red stock solution (500 µg/mL in acetone) into 1 mL of 75% glycerol (v/v in distilled water). A total of 15 µL of the prepared mixture was carefully applied onto the tissue section mounted on a microscope slide and evenly spread into one to three droplets. A cover glass was gently placed over the sample at an angle to prevent bubble formation. To seal the cover glass, the edges were coated with clear nail polish. The samples were analyzed using a Zeiss LSM 880 with Airyscan (NFEC-2016-05-209580) (Zeiss, Oberkochen, Germany)at Ewha Fluorescence Core Imaging Center.

2.4. ImageJ Analysis

ImageJ (ver. 1.54g) was employed to quantitatively analyze the image data by comparing the percentage of the stratum corneum area in each image. Based on the average thickness of the stratum corneum, four sections measuring 20 µm in thickness and 40 µm in length were selected per image (Figure 1A). The percentage of the area stained red within these sections was calculated and averaged to determine the overall percentage of the stratum corneum in each tissue sample (Figure 1B,C). The resulting measurements were then plotted on a graph.

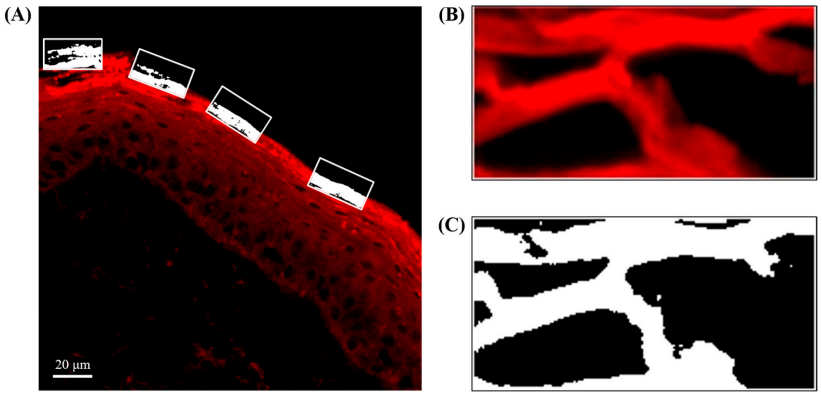


Figure 1. ImageJ analysis of epidermal lipid loss (**A**) The way to measure percentage of stratum corneum area. Four sample areas (20 µm × 40 µm) are picked on the image. (**B**) Sample area picked on the image. (**C**) Sample area edited with ImageJ. Nile red stained area appears white and ranges with no lipids appear black.

2.5. Transepidermal Water Loss (TEWL) Measurement

TEWL was measured using the GPSKIN Barrier PRO-II device (Gpower, Gyeonggi, Republic of Korea). During operation, the device was connected to the GPSKIN Research APP to record the measurements. Prior to measurement, tissues were placed in an open dish and equilibrated at room temperature and ambient humidity for 10 min. A probe adapter with a diameter of 0.7 cm was attached, and after pressing the start button without contacting the skin, the adapter was then placed in full contact with the measurement site for the period indicated by the program. The device determined TEWL by measuring changes in water vapor density inside the adapter during the measurement period, relative to the humidity detected at the start of the measurement.

2.6. Fluorescein Isothiocyanate (FITC)-Dextran Permeability Test

Minipig epidermis was subjected to the drying condition and incubated on media (DMEM high glucose with FBS (10%), Penicillin-Streptomycin (5%)), at 37 °C in a 5% CO_2 atmosphere for 24 h. After incubation, the tissue was removed, the media wiped off, and a 10 mm biopsy punch was used to excise a tissue sample. The sample was placed in a cell culture insert and secured with a silicone ring. Next, the insert was placed into each well of 6 well plates prefilled with 4 mL of PBS. The interior of the insert was then treated with 250 µL of 5 mg/mL FITC-Dextran (Sigma-Aldrich, 46944, Burlington, MA, USA) in PBS. The plate was covered with foil and maintained on a flat, non-shaking surface at room temperature. After 2 h, the insert was removed, and the receptor fluid was collected immediately. 150 µL of the receptor fluid was transferred into a clear-bottom 96-well black plate for fluorescence measurement at an excitation wavelength of 485 nm and an emission wavelength of 535 nm using a microplate reader (Infinite M200 Pro microplate reader (NFEC-2021-08-272460), Tecan Group Ltd., Mannedorf, Switzerland) equipped at Ewha Drug Development Research Core Center. The tissue removed from the insert was cryoprotected with an optimal cutting temperature (O.C.T.) compound, sectioned, and examined under a fluorescence microscope (Eclipse Ts2, Nikon, Tokyo, Japan) to assess the extent of FITC-Dextran penetration.

2.7. Statistics

Experimental values are presented as mean + SD. Data were analyzed using one-way ANOVA post hoc (Dunnett). p-values of 0.05 or less were considered significant. All data are presented as mean ± standard deviation (SD) from at least three independent experiments unless otherwise stated. Pearson correlation coefficients (r) were calculated to evaluate linear associations among the three indicators of stratum corneum (SC) barrier integrity: SC area (% of control), TEWL(g/hm^2), and FITC-Dextran penetration (ng/cm^2). All statistical analyses and correlation plots were generated using GraphPad Prism 5 (GraphPad Software, San Diego, CA, USA).

3. Results

3.1. Development of Dry Skin Models Using Isolated Minipig Epidermis

To induce dry skin conditions, isolated minipig epidermis was treated with various physical and chemical stressors, including the lipid-extracting solvent tert-butyl methyl ether (MTBE;100% for 1 or 5 min) and MTBE/Acetone (M/A; 50/50 for 1 or 5 min), the skin-irritating surfactant sodium dodecyl sulfate (SDS; 1% for 1 or 5 min), ultraviolet B (UVB) irradiation (30 mJ/cm^2), or tape stripping. The concentrations selected for the organic solvent conditions (MTBE and M/A) were observed to induce controlled SC disruption in in vitro skin models. The SDS concentration (1%) was chosen based on its widespread use in skin barrier evaluation assays as a standard condition for inducing barrier damage,

and was appropriate for application in this study. The resulting damage to the skin barrier and stratum corneum (SC) was then evaluated. To determine the most suitable condition for establishing a reproducible dry skin model for testing moisturizer efficacy, skin cross-sections from each treatment group were stained with Nile Red, visualized using confocal microscopy, and quantitatively analyzed using ImageJ (Figure 1).

In control tissues, SC measured approximately 15 µm in thickness and uniformly covered the epidermis, with no observable vacuolation or intercellular separation (Figure 2A). Tissues subjected to tape stripping exhibited extensive SC removal and exposure of the underlying viable epidermis. In chemically induced damage models, detachment and desquamation of the SC from the underlying layers were commonly observed, although the severity varied depending on the agent used and the duration of exposure. Among the tested treatments, 1% SDS caused more severe disruption of the SC compared to either MTBE or M/A. Additionally, a 5 min exposure to 1% SDS resulted in greater SC damage than a 1 min treatment. The area of Nile Red-stained SC was quantified using ImageJ and compared to the untreated control (Figure 2B). Of all tested conditions, treatment with M/A for 5 min produced approximately 50% reduction in SC area, with minimal inter-sample variability, suggesting that it offers a consistent and reproducible model for barrier disruption.

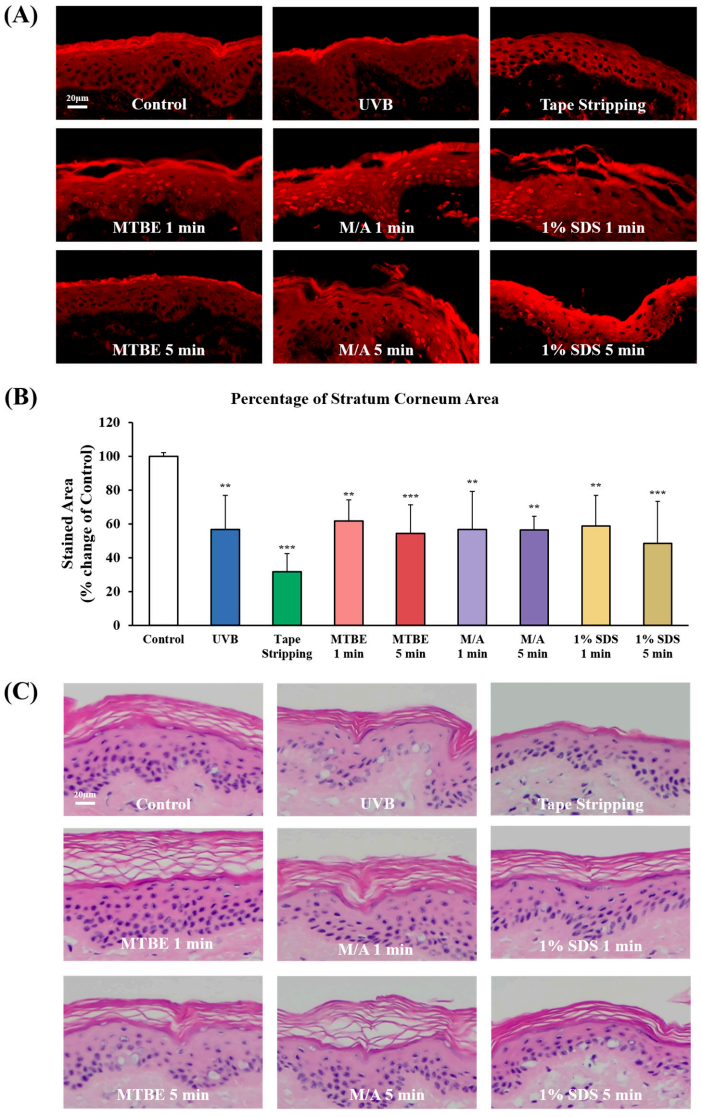


Figure 2. Effects of dry skin stimuli on minipig epidermis. (**A**) Minipig epidermis subjected to drying stimuli were sectioned to a thickness of less than 10 µm, mounted on glass slides, and stained with

Nile red. Fluorescence images were captured at 40× magnification. The scale bar represents 20 μm. (**B**) The graph quantifies the stratum corneum area measured from the fluorescence images. Data are presented as mean + SD (N = 5). Statistical significance was determined using one-way ANOVA. (** $p < 0.01$, *** $p < 0.001$). (**C**) Minipig skins treated with dry conditions were microscopically imaged after H&E staining. Images were captured at 10× magnification. The scale bar represents 20 μm.

Additionally, hematoxylin and eosin (H&E) staining was performed on tissue cross-sections to verify the structural alterations in the SC observed in Nile Red fluorescence analysis (Figure 2C). Tissues subjected to tape stripping exhibited the thinnest SC layer, indicating that most of the SC had been removed. In tissues treated with MTBE for 1 min or M/A for 5 min, enlarged intercellular voids and a net-like appearance were observed within the SC, suggesting solvent-induced lipid extraction and subsequent delamination of SC layers. Taken together, data from both fluorescence microscopy and H&E staining indicate that treatment with M/A for 5 min provides optimal and reproducible conditions for inducing controlled SC disruption and skin barrier impairment.

3.2. Evaluation of Skin Barrier Function in Dry Skin Models

Dry skin is typically characterized by impaired barrier function, which can be assessed by elevated TEWL and increased percutaneous penetration of external substances. To evaluate the functional integrity of the skin barrier in our dry skin models, TEWL and percutaneous absorption of 4 kDa FITC-dextran were measured. Prior to TEWL assessment, the treated skin samples were incubated for 24 h at 37 °C in a 5% CO_2 atmosphere to simulate physiological recovery conditions. After incubation, tissues were equilibrated at room temperature and ambient humidity for 10 min before TEWL measurement.

All treatment groups subjected to skin-damaging conditions exhibited significantly higher TEWL values compared to the untreated control group (mean TEWL: 13.22) (Figure 3A). With the exception of the UVB (30 mJ/cm^2) and MTBE (1 min) treatment groups, the remaining six experimental conditions showed comparable TEWL values ranging from 20.7 to 22.3. These results confirm that SC damage induced by chemical or mechanical insults is consistently associated with compromised barrier function.

We also assessed changes in skin permeability using 4 kDa FITC-dextran, a macromolecule that does not penetrate intact skin due to its high molecular weight. However, when the skin barrier is compromised, FITC-dextran permeability increases significantly [36,39]. As expected, the control group exhibited minimal FITC-dextran penetration (Figure 3B), while tissues subjected to skin-damaging conditions showed significantly increased permeation. Notably, UVB exposure (30 mJ/cm^2) and M/A treatment for 5 min produced the most consistent increases in FITC-dextran permeability.

Visual examination of FITC-dextran distribution using fluorescence microscopy (Figure 3C) further supported these findings. In the control group, FITC fluorescence was faint and largely confined to the SC and upper epidermal layers. In contrast, tissues treated with 1% SDS for 5 min exhibited strong, widespread FITC fluorescence, indicating pronounced barrier disruption and elevated permeability. Other treatment groups—including 100% MTBE for 5 min, M/A for 1 and 5 min, and 1% SDS for 1 min—showed intermediate levels of FITC penetration. While these were lower than the 1% SDS 5 min group, they were clearly elevated compared to the control, confirming partial barrier compromise.

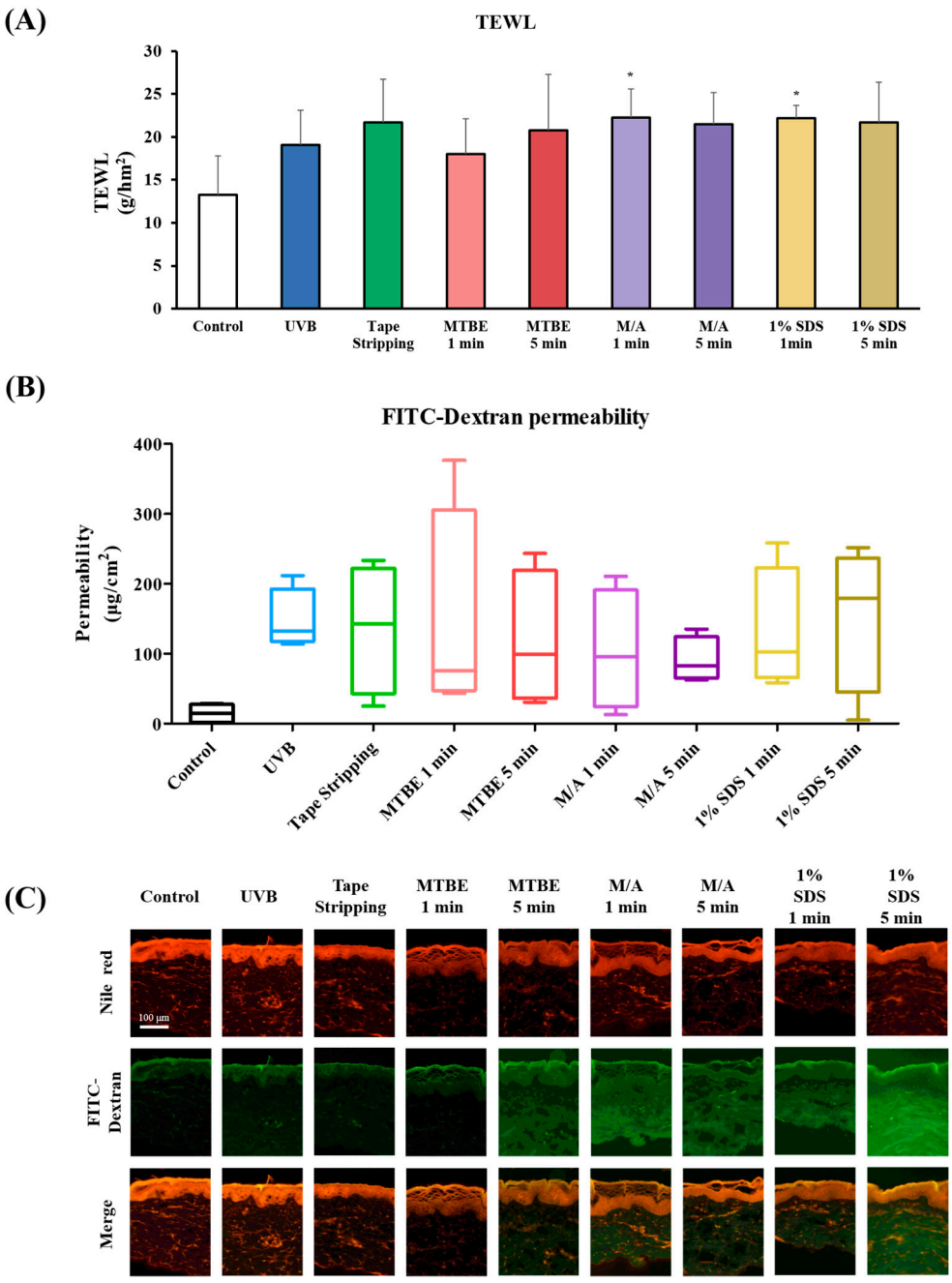


Figure 3. Skin barrier function of minipig epidermis dry skin models (**A**) The graph presents TEWL changes under drying conditions relative to the control. Tissues were subjected to skin drying conditions, followed by stabilization prior to measurement. Data are expressed as mean + SD (N = 4). Statistical significance was determined using one-way ANOVA (* $p < 0.05$). (**B**) The permeability of 4 kDa FITC-Dextran was assessed by fluorescence measurement of the receptor fluid. Fluorescence was recorded at an excitation wavelength of 485 nm and an emission wavelength of 535 nm. Data are presented as individual values with mean (N = 4). Statistical significance was determined using one-way ANOVA. (**C**) Cross-sectional images of representative tissues were selected based on values closest to the mean permeability for each drying condition. Tissues were cryo-sectioned, stained with Nile red, and observed under a fluorescence microscope. Two fluorescence images were merged to visualize the extent of permeability. Images were captured at 10× magnification. Scale bar represents 100 µm.

3.3. Correlation of Dry Skin Parameters in the Minipig Epidermis Model

To identify the most reproducible and informative parameter for characterizing the dry skin model, correlation analyses were performed among the three measured endpoints: SC area (expressed as % of control), TEWL, and FITC-dextran skin penetration (ng/cm^2) (Figure 4). Pearson correlation analysis revealed a strong inverse correlation between SC area and TEWL (r = −0.85, p = 0.004), as well as between SC area and FITC-dextran penetration (r = −0.81, p = 0.008). A positive correlation was also observed between TEWL and FITC-dextran penetration (r = 0.66), though it did not reach statistical significance (p = 0.052).

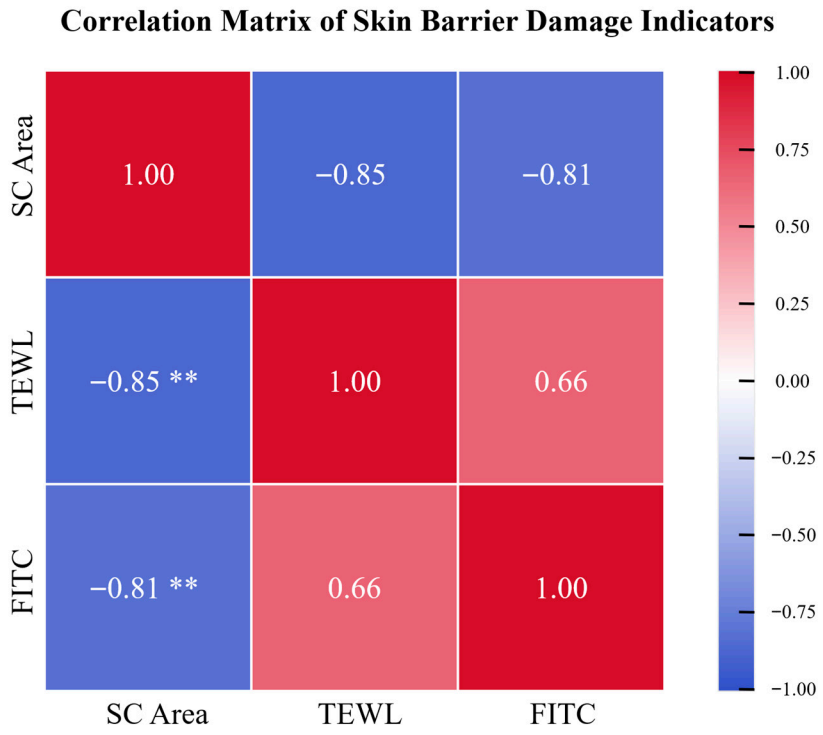


Figure 4. Correlation analysis for the skin barrier parameters in minipig epidermis dry skin models. Heatmap demonstrate the relationships between SC area (% of control), TEWL, and FITC-Dextran penetration. Pearson correlation coefficients (r) and corresponding p-values were as follows: SC area vs. TEWL: r = −0.85, p = 0.004; SC area vs. FITC-Dextran: r = −0.81, p = 0.008; TEWL vs. FITC-Dextran: r = 0.66, p = 0.052 (** p < 0.01).

These findings suggest that quantification of SC area based on fluorescence imaging can serve as a reliable, objective indicator of skin barrier damage. This parameter may be particularly useful for evaluating the severity of dry skin conditions and the efficacy of moisturizing treatments.

3.4. MTBE/Acetone-Induced Dry Skin Model Using Human Cadaver Skin Tissue

Based on the extent and reproducibility of SC and barrier damage, treatment with M/A for 5 min was identified as the optimal condition for inducing dry skin in the minipig epidermis model. To assess whether this condition could similarly induce dry skin features in human skin, we applied the same treatment to commercially obtained human cadaver skin tissues.

As shown in Figure 5, treatment with M/A for 5 min produced a comparable pattern of SC disruption in human cadaver skin as observed in minipig epidermis. In particular, SC desquamation was evident, and a net-like separation of the SC layers was observed, consistent with the characteristic damage pattern induced by lipid extraction. However,

the human SC was notably thicker than that of minipig skin, and complete detachment of the SC was not observed. This suggests that the human epidermis may possess greater resistance to chemical-induced barrier disruption, potentially due to structural differences in SC architecture.

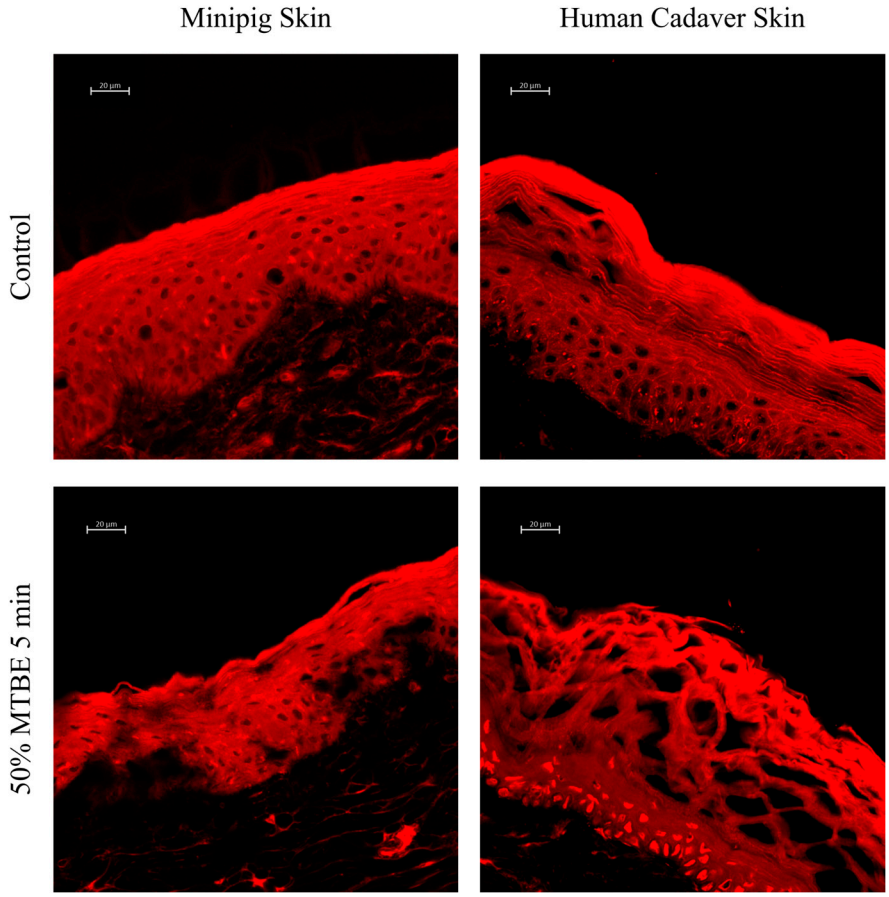


Figure 5. Comparison of MTBE-induced dry skin model in minipig epidermis and human cadaver skin. M/A were applied to minipig epidermis or human cadaver skin for 5 min as skin drying condition. Treated skin tissues were sectioned to a thickness of less than 10 µm, mounted on glass slides, and stained with Nile red. Fluorescence images were captured at 40× magnification. The scale bar represents 20 µm.

4. Discussion

In this study, we developed an in vitro dry skin model using isolated minipig epidermis and human cadaver skin. Skin barrier damage was assessed morphologically by quantifying the SC area using fluorescence imaging of Nile Red-stained tissue sections. Importantly, functional impairment of the barrier was evaluated through TEWL and the percutaneous permeability of 4 kDa FITC-dextran. Our findings demonstrated that skin-drying stimuli induced SC disruption, lipid loss, increased TEWL, and enhanced permeability in both minipig and human skin models. These morphological and functional alterations closely mirror changes observed in vivo and in human dry skin conditions [13,14,40,41].

In the minipig epidermis model, SC area showed a strong inverse correlation with both TEWL and FITC-dextran penetration, whereas the positive correlation between TEWL and FITC-dextran was less evident. This discrepancy likely reflects differences in the barrier properties measured by each assay. TEWL quantifies water loss through the stratum corneum, while FITC-dextran penetration evaluates the passage of larger hydrophilic molecules. Because these parameters assess distinct aspects of barrier integrity, perfect correlation is not expected. Image-based SC analysis produced a clearer negative correlation

even with a small sample size, whereas both TEWL and FITC-dextran values increased with barrier disruption, making their relationship more susceptible to variability.

Comparison of minipig and human cadaver skin under the same drying condition revealed distinct structural responses and barrier dysfunction, reflecting differences in skin thickness and resistance between species. We acknowledge that this limits the translational generalization of our findings. Future studies will therefore extend the comparison to a wider range of concentrations and exposure times, including stronger damage conditions, to optimize the human tissue model and establish a more robust basis for cross-species validation.

The skin is continuously exposed to environmental stressors that can impair the epidermal barrier [18,42]. Both physical and chemical insults compromise SC integrity, particularly its lipid architecture, resulting in elevated TEWL and diminished hydration. Reduced moisture levels may also lead to abnormally accelerated desquamation [43]. For example, common personal care products such as soaps and cleansers have been shown to deplete SC lipids and induce dryness [44,45]. Ultraviolet (UV) irradiation further contributes to barrier dysfunction and accelerates photoaging [46,47], while mechanical stressors—such as scratching and friction—are frequent contributors to barrier damage [48]. To mimic these real-world conditions, experimental models have employed strategies such as detergent-induced lipid extraction, tape stripping, and UV exposure [18,20,49].

Traditionally, the efficacy of moisturizers has been evaluated using animal models or human trials with finished products. However, increasing global restrictions on animal testing in the cosmetics industry now preclude in vivo animal assays. Moreover, in vitro cell-based assays are often unsuitable for testing viscous and waxy formulations due to poor applicability. While ex vivo models using human or porcine skin have been explored, many of these rely solely on TEWL measurements. Given TEWL's sensitivity to external environmental conditions, generating reproducible data remains a challenge.

In this context, our model addresses a critical unmet need by providing a reliable, reproducible, and ethically compliant platform to assess the efficacy of moisturizing agents prior to human testing. The model recapitulates key morphological and functional features of dry skin, offering dual assessment through structural imaging and functional measurements. High-resolution visualization of SC damage complements quantitative data, enabling a deeper understanding of the mechanisms through which moisturizers exert their effects—information that cannot be easily obtained from human trials alone.

However, some limitations exist in our model. Our model cannot assess moisturizing-related genes, which is a critical factor in achieving moisturizing efficacy. This point shall be supplemented with cell-based assay or ex vivo life skin models [50]. Furthermore, we have not assessed whether our model can be actually applied in evaluating the moisturizing effects of various cosmetic ingredients. For the practical implementation of the model in the evaluation of moisturizing effects of new cosmetic ingredients, a future validation process shall be necessary to test the applicability of our model for various types of reference substances with known moisturizing efficacy and the intra- and inter-laboratory reproducibility.

In summary, we present a novel in vitro dry skin model incorporating both minipig and human skin tissues, capable of simultaneously assessing morphological and functional barrier impairment. This model represents a valuable tool to accelerate the development and screening of new skin moisturizers under ethically and scientifically robust conditions.

Author Contributions: Conceptualization, J.-W.C. and K.-M.L.; methodology, J.-W.C., K.L. and B.-G.K.; formal analysis, J.-W.C., B.-G.K. and J.-h.H.; investigation, J.-W.C., B.-G.K. and J.-h.H.; resources, K.L. and K.-M.L.; data curation, J.-W.C. and B.-G.K.; writing—original draft preparation, J.-W.C. and B.-G.K.; writing—review and editing, K.-M.L.; supervision, K.-M.L.; project administration, K.-M.L.; funding acquisition, K.L. and K.-M.L. All authors have read and agreed to the published version of the manuscript.

Funding: This work was funded by grants from the Korea Environment Industry and Technology Institute (KEITI) through the Technology Program for Establishing Biocide Safety Management funded by the Ministry of Environment Korea (RS-2025-02223356) and Korea Health Technology R&D Project through the Korea Health Industry Development Institute (KHIDI), funded by the Ministry of Health and Welfare Korea (RS-2023-KH14129).

Institutional Review Board Statement: Pig skin epidermis was obtained from a company that has received ethical approval from the Ethical Committee of AUPRES-IACUC (Approval No.: AUPRES-IACUC 250414-002; Approval Date: 25.04.2024). Therefore, the ethical approval is not applicable. The human skin membrane was acquired from a vendor who stated that the skin was donated as a gift by a deceased individual with body donation registration documents, in accordance with Oregon state law, USA. Therefore, the ethical approval is not applicable.

Informed Consent Statement: The human skin membrane was acquired from a vendor who stated that the skin was donated as a gift by a deceased individual with body donation registration documents, in accordance with Oregon state law, USA. Therefore, the ethical approval is not applicable.

Data Availability Statement: The data presented in this study are available on request from the corresponding author.

Conflicts of Interest: The authors declare no conflicts of interest.

References

1. Thakur, A.; Shah, D.; Rai, D.; Parra, D.C.; Pathikonda, S.; Kurilova, S.; Cili, A. Therapeutic values of exosomes in cosmetics, skin care, tissue regeneration, and dermatological diseases. *Cosmetics* **2023**, *10*, 65. [CrossRef]
2. Mawazi, S.M.; Ann, J.; Othman, N.; Khan, J.; Alolayan, S.O.; Al thagfan, S.S.; Kaleemullah, M. A review of moisturizers; history, preparation, characterization and applications. *Cosmetics* **2022**, *9*, 61. [CrossRef]
3. Ueda, Y.; Murakami, Y.; Saya, Y.; Matsunaka, H. Optimal application method of a moisturizer on the basis of skin physiological functions. *J. Cosmet. Dermatol.* **2022**, *21*, 3095–3101. [CrossRef]
4. Liu, J.-K. Natural products in cosmetics. *Nat. Prod. Bioprospecting* **2022**, *12*, 40. [CrossRef] [PubMed]
5. Bhat, B.B.; Kamath, P.P.; Chatterjee, S.; Bhattacherjee, R.; Nayak, U.Y. Recent updates on nanocosmeceutical skin care and anti-aging products. *Curr. Pharm. Des.* **2022**, *28*, 1258–1271. [CrossRef]
6. Danby, S.G.; Andrew, P.V.; Taylor, R.N.; Kay, L.J.; Chittock, J.; Pinnock, A.; Ulhaq, I.; Fasth, A.; Carlander, K.; Holm, T. Different types of emollient cream exhibit diverse physiological effects on the skin barrier in adults with atopic dermatitis. *Clin. Exp. Dermatol.* **2022**, *47*, 1154–1164. [CrossRef] [PubMed]
7. Kang, S.-Y.; Um, J.-Y.; Chung, B.-Y.; Lee, S.-Y.; Park, J.-S.; Kim, J.-C.; Park, C.-W.; Kim, H.-O. Moisturizer in patients with inflammatory skin diseases. *Medicina* **2022**, *58*, 888. [CrossRef]
8. Shindo, S.; Murota, H.; Seki, T.; Mori, K.; Kaizu, K.; Nishizaka, T.; Takagi, Y.; Katayama, I. Effects of a moisturizer containing pseudo-ceramide and a eucalyptus extract on sweating function in adult atopic dermatitis: A double-blind, randomized, controlled left-right comparison clinical trial. *J. Cosmet. Dermatol.* **2022**, *21*, 4503–4509. [CrossRef]
9. Ainurofiq, A.; Haya, A.F.F.D.; Safitri, A.N.; Solihatin, I.Z.; Nusriya, S.B.; Nugroho, T.S. Characterization and application of moisturizer in skin treatment: A review: Moisturizer in Skin Treatment. *J. Pak. Assoc. Dermatol.* **2023**, *33*, 1602–1613.
10. Chandan, N.; Rajkumar, J.R.; Shi, V.Y.; Lio, P.A. A new era of moisturizers. *J. Cosmet. Dermatol.* **2021**, *20*, 2425–2430. [CrossRef] [PubMed]
11. Alam, S.; Algahtani, M.S.; Ahmad, M.Z.; Ahmad, J. Investigation utilizing the HLB concept for the development of moisturizing cream and lotion: In-vitro characterization and stability evaluation. *Cosmetics* **2020**, *7*, 43. [CrossRef]
12. Pavlou, P.; Siamidi, A.; Varvaresou, A.; Vlachou, M. Skin care formulations and lipid carriers as skin moisturizing agents. *Cosmetics* **2021**, *8*, 89. [CrossRef]
13. Del Rosso, J.; Zeichner, J.; Alexis, A.; Cohen, D.; Berson, D. Understanding the epidermal barrier in healthy and compromised skin: Clinically relevant information for the dermatology practitioner: Proceedings of an expert panel roundtable meeting. *J. Clin. Aesthetic Dermatol.* **2016**, *9*, S2.
14. Harding, C.R. The stratum corneum: Structure and function in health and disease. *Dermatol. Ther.* **2004**, *17*, 6–15. [CrossRef]
15. Misra, M.; Ananthapadmanabhan, K. changes in epidermis and transepidermal water loss. *J. Soc. Cosmet. Chem.* **1997**, *48*, 219–234.
16. Ananthapadmanabhan, K.; Mukherjee, S.; Chandar, P. Stratum corneum fatty acids: Their critical role in preserving barrier integrity during cleansing. *Int. J. Cosmet. Sci.* **2013**, *35*, 337–345. [CrossRef]

17. Rajkumar, J.; Chandan, N.; Lio, P.; Shi, V. The skin barrier and moisturization: Function, disruption, and mechanisms of repair. *Ski. Pharmacol. Physiol.* **2023**, *36*, 174–185. [CrossRef]
18. Biniek, K.; Levi, K.; Dauskardt, R.H. Solar UV radiation reduces the barrier function of human skin. *Proc. Natl. Acad. Sci. USA* **2012**, *109*, 17111–17116. [CrossRef]
19. Panich, U.; Sittithumcharee, G.; Rathviboon, N.; Jirawatnotai, S. Ultraviolet radiation-induced skin aging: The role of DNA damage and oxidative stress in epidermal stem cell damage mediated skin aging. *Stem Cells Int.* **2016**, *2016*, 7370642. [CrossRef] [PubMed]
20. Gao, Y.; Wang, X.; Chen, S.; Li, S.; Liu, X. Acute skin barrier disruption with repeated tape stripping: An in vivo model for damage skin barrier. *Ski. Res. Technol.* **2013**, *19*, 162–168. [CrossRef] [PubMed]
21. Keurentjes, A.J.; Jakasa, I.; Kezic, S. Research techniques made simple: Stratum corneum tape stripping. *J. Investig. Dermatol.* **2021**, *141*, 1129–1133.e1. [CrossRef]
22. Danby, S.G.; Andrew, P.V.; Brown, K.; Chittock, J.; Kay, L.J.; Cork, M.J. An investigation of the skin barrier restoring effects of a cream and lotion containing ceramides in a multi-vesicular emulsion in people with dry, eczema-prone, skin: The RESTORE study phase 1. *Dermatol. Ther.* **2020**, *10*, 1031–1041. [CrossRef]
23. Draelos, Z.D.; Diaz, I.; Namkoong, J.; Wu, J.; Boyd, T. Efficacy evaluation of a topical hyaluronic acid serum in facial photoaging. *Dermatol. Ther.* **2021**, *11*, 1385–1394. [CrossRef] [PubMed]
24. Wang, D.-Q.; Li, X.; Zhang, R.-Y.; Yuan, C.; Yan, B.; Humbert, P.; Quan, Z.-X. Effects of investigational moisturizers on the skin barrier and microbiome following exposure to environmental aggressors: A randomized clinical trial and ex vivo analysis. *J. Clin. Med.* **2023**, *12*, 6078. [CrossRef] [PubMed]
25. Koseki, K.; Kawasaki, H.; Atsugi, T.; Nakanishi, M.; Mizuno, M.; Naru, E.; Ebihara, T.; Amagai, M.; Kawakami, E. Assessment of skin barrier function using skin images with topological data analysis. *npj Syst. Biol. Appl.* **2020**, *6*, 40. [CrossRef]
26. Qassem, M.; Kyriacou, P. Review of modern techniques for the assessment of skin hydration. *Cosmetics* **2019**, *6*, 19. [CrossRef]
27. Rogiers, V. EEMCO guidance for the assessment of transepidermal water loss in cosmetic sciences. *Ski. Pharmacol. Physiol.* **2001**, *14*, 117–128. [CrossRef]
28. Wu, Y.; Ran, J.; Tanaka, T.; Liu, Q. Quantitative skin surface hydration measurement by visible optical image processing: A pilot study. *Ski. Res. Technol.* **2024**, *30*, e13773. [CrossRef] [PubMed]
29. Hong, S.; Maitra, P.; Nguyen, A.; Kadoya, K.; Mehta, R.C. Development of an in vitro Functional Assay to Evaluate the Occlusive Properties of Moisturizers on Dry Skin. *Ski. Pharmacol. Physiol.* **2023**, *36*, 140–148. [CrossRef]
30. Uehara, O.; Kusuhara, T.; Nakamura, T. Transepidermal water loss estimation model for evaluating skin barrier function. *Adv. Biomed. Eng.* **2023**, *12*, 1–8. [CrossRef]
31. Gibbsa, M.P.S.; Boelsmaa, G.P.E.; Koertenb, H.; Mommaasa, J.B.M. Barrier function in reconstructed epidermis and its resemblance to native human skin. *Ski. Pharmacol. Appl. Ski. Physiol.* **2001**, *14*, 63–71.
32. Barthe, M.; Clerbaux, L.-A.; Thénot, J.-P.; Braud, V.M.; Osman-Ponchet, H. Systematic characterization of the barrier function of diverse ex vivo models of damaged human skin. *Front. Med.* **2024**, *11*, 1481645. [CrossRef]
33. Hwang, J.-h.; Jeong, H.; Lee, N.; Hur, S.; Lee, N.; Han, J.J.; Jang, H.W.; Choi, W.K.; Nam, K.T.; Lim, K.-M. Ex vivo live full-thickness porcine skin model as a versatile in vitro testing method for skin barrier research. *Int. J. Mol. Sci.* **2021**, *22*, 657. [CrossRef] [PubMed]
34. Mojumdar, E.H.; Madsen, L.B.; Hansson, H.; Taavoniku, I.; Kristensen, K.; Persson, C.; Morén, A.K.; Mokso, R.; Schmidtchen, A.; Ruzgas, T. Probing skin barrier recovery on molecular level following acute wounds: An in vivo/ex vivo study on pigs. *Biomedicines* **2021**, *9*, 360. [CrossRef]
35. Uhm, C.; Jeong, H.; Lee, S.H.; Hwang, J.S.; Lim, K.M.; Nam, K.T. Comparison of structural characteristics and molecular markers of rabbit skin, pig skin, and reconstructed human epidermis for an ex vivo human skin model. *Toxicol. Res.* **2023**, *39*, 477–484. [CrossRef]
36. Hong, J.-h.; Lim, K.-M. Development of skin corrosion and irritation test methods employing ex vivo porcine skin model. *Toxicol. Vitr.* **2025**, *106*, 106055. [CrossRef] [PubMed]
37. Jung, Y.O.; Jeong, H.; Cho, Y.; Lee, E.O.; Jang, H.W.; Kim, J.; Nam, K.; Lim, K.M. Lysates of a Probiotic, Lactobacillus rhamnosus, Can Improve Skin Barrier Function in a Reconstructed Human Epidermis Model. *Int. J. Mol. Sci.* **2019**, *20*, 4289. [CrossRef]
38. McDaniel, D.H.; Dover, J.S.; Wortzman, M.; Nelson, D.B. In vitro and in vivo evaluation of a moisture treatment cream containing three critical elements of natural skin moisturization. *J. Cosmet. Dermatol.* **2020**, *19*, 1121–1128. [CrossRef]
39. Tu, Y.; Wang, L.; An, L.; He, L. Hsa-miR-31-3p targets CLDN8 to compromise skin barrier integrity in psoriasis. *Biochem. Biophys. Rep.* **2025**, *42*, 101976. [CrossRef] [PubMed]
40. Lee, H.-J.; Lee, S.-H. Epidermal permeability barrier defects and barrier repair therapy in atopic dermatitis. *Allergy Asthma Immunol. Res.* **2014**, *6*, 276–287. [CrossRef]
41. Levi, K.; Weber, R.; Do, J.; Dauskardt, R. Drying stress and damage processes in human stratum corneum. *Int. J. Cosmet. Sci.* **2010**, *32*, 276–293. [CrossRef]

42. Sözener, Z.C.; Cevhertas, L.; Nadeau, K.; Akdis, M.; Akdis, C.A. Environmental factors in epithelial barrier dysfunction. *J. Allergy Clin. Immunol.* **2020**, *145*, 1517–1528. [CrossRef] [PubMed]
43. Hashizume, H. Skin aging and dry skin. *J. Dermatol.* **2004**, *31*, 603–609. [CrossRef]
44. Boyce, J.M.; Kelliher, S.; Vallande, N. Skin irritation and dryness associated with two hand-hygiene regimens: Soap-and-water hand washing versus hand antisepsis with an alcoholic hand gel. *Infect. Control Hosp. Epidemiol.* **2000**, *21*, 442–448. [CrossRef]
45. Slotosch, C.M.; Kampf, G.; Löffler, H. Effects of disinfectants and detergents on skin irritation. *Contact Dermat.* **2007**, *57*, 235–241. [CrossRef]
46. Li, Z.; Jiang, R.; Wang, M.; Zhai, L.; Liu, J.; Xu, X.; Sun, L.; Zhao, D. Ginsenosides repair UVB-induced skin barrier damage in BALB/c hairless mice and HaCaT keratinocytes. *J. Ginseng Res.* **2022**, *46*, 115–125. [CrossRef] [PubMed]
47. Tanaka, Y.; Uchi, H.; Furue, M. Antioxidant cinnamaldehyde attenuates UVB-induced photoaging. *J. Dermatol. Sci.* **2019**, *96*, 151–158. [CrossRef] [PubMed]
48. Furue, K.; Ulzii, D.; Tanaka, Y.; Ito, T.; Tsuji, G.; Kido-Nakahara, M.; Nakahara, T.; Furue, M. Pathogenic implication of epidermal scratch injury in psoriasis and atopic dermatitis. *J. Dermatol.* **2020**, *47*, 979–988. [CrossRef]
49. Held, E.; Lund, H.; Agner, T. Effect of different moisturizers on SLS-irritated human skin. *Contact Dermat.* **2001**, *44*, 229–234. [CrossRef]
50. Hwang, J.H.; Kang, Y.; Park, H.J.; Kim, S.; Lee, S.H.; Kim, H.; Nam, S.J.; Lim, K.M. Skin wound healing effects of (+)-syringaresinol from ginseng berry. *J. Ginseng Res.* **2023**, *47*, 654–661. [CrossRef]

Disclaimer/Publisher's Note: The statements, opinions and data contained in all publications are solely those of the individual author(s) and contributor(s) and not of MDPI and/or the editor(s). MDPI and/or the editor(s) disclaim responsibility for any injury to people or property resulting from any ideas, methods, instructions or products referred to in the content.